Cyber Defense of Rotating Machinery Using an Integrated 'Fuse' Bearing

Evyatar Cohen[1], Jacob Bortman[2] and Renata Klein[3]

[1,2] *Pearlstone Center for Aeronautical Engineering Studies and Laboratory for Mechanical Health Monitoring, Department of Mechanical Engineering, Ben-Gurion University of the Negev, P.O. Box 653, Beer Sheva 84105, Israel.*

cohenave1@gmail.com
jacbort@gmail.com

[3]*R.K. Diagnostics, Gilon, P.O.B. 101, D.N. Misgav 20103, Israel*
Renata.Klein@RKDiagnostics.co.il

ABSTRACT

A new concept is proposed for protection against cyber-attacks aiming to create excessive loads that will eventually result in irreversible damage to critical rotating machines. This novel approach is used as an additional defense layer of cyber protection to prevent hostile entities from breaking into the control system of the critical machines.

A relatively small bearing is used as the "weak link", or the "fuse" mechanism, in the critical system. This mechanism allows rapid life degradation under harmful regimes, which leads to early detection of attack and finally to prevention of catastrophic damage to a critical machine. The detection of the fuse degradation process is based on techniques of machine health monitoring via vibrations signatures.

An analytical model was developed, allowing to design the 'fuse bearing'. The model examines the response of the fuse bearing, through its life degradation rate, by simulating a wide range of attack scenarios. The model integrates sub models: bearing life estimation models and a dynamic response of mechanical rotating machines model. In addition, a set of fatigue life experiments were conducted on a designated experimental test facility with the purpose of proving the early damage detection ability of the fuse bearing using vibration analysis.

1. INTRODUCTION

Many mechanical facilities in industry are defined as "critical", such as turbines in power plants, centrifuges for uranium enrichment, big pumps in water companies, etc. These machines work many hours continuously, and therefore require careful maintenance. These facilities are designed to work at limited regimes of speeds and loads. However, exceeding these regimes can lead to failures created by fatigue and rubbing, and finally to catastrophic damage and destruction.

Industries tend to operate these machines in safe conditions and try to extend the machine lives by frequent maintenance. Usually, these machines are controlled by a control system that help provide better supervision. These "critical" machines are strategic targets of different kinds of cyber-attacks. Most of the attacks try to damage the mechanical parts and cause irreversible damage. So far, most protection mechnism are based on software and firewalls trying to prevent the penetration of harmful elements into control systems. But in some cases, these protections are not enough.

In this research, a new concept is proposed for mechanical protection against cyber-attacks on critical rotating machines (Figure 1). The proposed approach integrates a fuse mechanism into the critical rotating machine. This fuse mechanism is simply a relatively small ball bearing, designed to be the weakest component in the machine. It is expected that under attack or abuse, the fuse mechanism will be damaged first, ahead of the other critical components of the machine. In this case, the fast life degradation and early failure will lead to early detection of attack and finally to the prevention of catastrophic damage to a critical machine.

The detection process of fuse bearing failure caused by cyber-attack is based on techniques of machine health monitoring via vibrations signatures. Advanced signal processing and feature extraction methodologies are applied for initial failure detection and degradation tracking.

As a part of this research, an analytical model simulating the wear and failure of a fuse bearing under a wide range of attack scenarios was developed. Statistical models for bearing life estimation were used to build this model. The proposed

model helped us to design and to analyze the fuse system. Actually, life prediction and degradation simulations of the fuse bearing and the machine critical bearings at each attack scenario were performed, in order to define the proper requirements for an effective fuse system. As described in the conceptual diagram (Figure 1), an external load can be applied onto a fuse bearing with load level control set by a function (defined as a "Transfer Function", TF) of some attack parameters. This external load helps to accelerate life degradation and failure of the fuse bearing in case of attack. To reduce the possibility of taking over the fuse system by hostile elements, it is designed to operate autonomously and it is not controlled by a computer. Three optional TF's are examined and discussed in order to find the optimal TF that brings the fastest fuse life degradation rate for specific attack simulations.

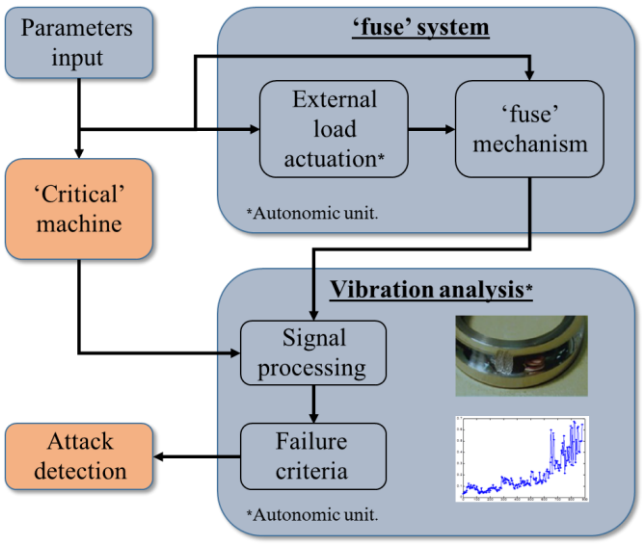

Figure 1. System defense scheme concept.

The regime of a critical rotating machine is defined by a set of parameters that are usually under supervision of a control system (for example, rotating speed). In terms of a cyber-attack, these parameters are called "parameters of attack". It is assumed that the attacker controls these parameters maliciously to bring the critical system to harmful regimes. Also, the parameters of attack may vary with time. Hence, the chosen bearing life models are applicable for variable operating conditions.

Endurance experiments were conducted on a fuse bearing, in a test facility that was designed for this research in the lab. These experiments were designed to test the feasibility of the protection by the fuse mechanism concept, i.e. to prove the ability to cause the fuse bearing failure and to detect early the damage through vibration analysis (to define the appropriate condition indicators). This paper focus mainly on the model development and the presentation of simulation results. The experiments of the fuse bearing fatigue life tests are still carried out, so the results and discussion on the applied signal analysis techniques will be presented separately.

2. MODEL DESCRIPTION

In this chapter, a model that allows the running of multiple simulations of attack on a critical rotating machine and simulates its dynamic behavior and its effect on bearing fatigue, is presented. In addition, the model helps to design the fuse system and to analyze its efficiency at multiple attack scenarios. Please note that high efficacy of a fuse system is expressed as fast mechanical life degradation of the fuse bearing during an attack (which is estimated by life models), relative to the degradation rate at normal operation. A block diagram showing the structure of the overall model is depicted in Figure 2.

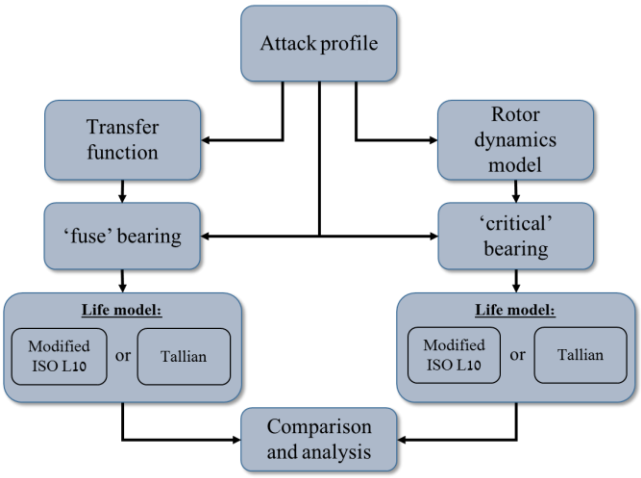

Figure 2. Model block diagram.

Mathematical expressions and models that describe each block in Figure 2 are listed and detailed in the next sections.

2.1. Critical rotating machine dynamics modeling

A dynamic model of a rotating machine with a single mass rotor (Meirovitch, 2001), which appears as the "rotor dynamics model" block in Figure 2, is described in this section. A critical rotating machine is assumed to involve a heavy rotating disk, known as a rotor, attached to a flexible shaft mounted on rigid bearings. Typical examples are turbines, compressors, centrifuges, etc. It is assumed that the rotor has some eccentricity and, as a result, the rotation produces a centrifugal force causing the shaft to bend. For certain rotational velocities, the system experiences violent vibrations. Figure 3 shows a shaft rotating with angular velocity ω. The shaft carries a disk of total mass m and is assumed to be massless. Hence, the motion of the system can be described by the displacements x and y of geometric center S of the disk.

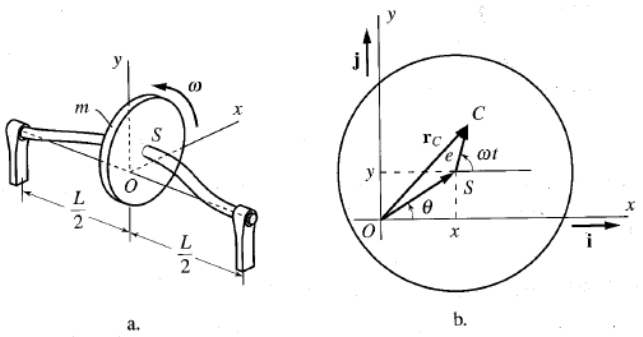

Figure 3. Dynamic rotating machine. (a) A rotor mounted on a shaft and supported by rigid bearings; (b) Mass center C and geometric center S, relative to origin. (Meirovitch, 2001).

The equations of motion in x and y directions, as depicted in Meirovitch's book, can be described as follows:

$$\begin{aligned} \ddot{x} + 2\zeta_x \omega_n \dot{x} + \omega_{nx}^2 x &= e\omega^2 \cos(\omega t) \\ \ddot{y} + 2\zeta_y \omega_n \dot{y} + \omega_{ny}^2 y &= e\omega^2 \sin(\omega t) \end{aligned} \quad (1)$$

The most common case is that the shaft stiffness is the same in both directions, $k_x = k_y = k$. In this case, the two natural frequencies coincide and so do the viscous damping factors:

$$\zeta_x = \zeta_y = \zeta = \frac{c}{2m\omega_n}; \quad \omega_{nx} = \omega_{ny} = \omega_n = \sqrt{\frac{k}{m}} \quad (2)$$

Since the equations of motion are linear and not coupled, the solution in both directions is:

$$\begin{aligned} x(t) &= |X(\omega)| \cos(\omega t - \phi) \\ y(t) &= |Y(\omega)| \sin(\omega t - \phi) \end{aligned} \quad (3)$$

$|X(\omega)|$, $|Y(\omega)|$ and ϕ are detailed in Appendix A. As a result of $x(t)$ and $y(t)$ motions, the bearing reactions, according to Newton's second law, are described as:

$$\begin{aligned} F_x &= m\ddot{x}/2 \\ &= m\omega^2\{|X(\omega)| \cos(\omega t - \phi) + e \cdot \cos(\omega t)\}/2 \\ F_y &= m\ddot{y}/2 \\ &= m\omega^2\{|Y(\omega)| \sin(\omega t - \phi) + e \cdot \sin(\omega t)\}/2 \end{aligned} \quad (4)$$

The equivalent load amplitude can be defined as:

$$F_{OS} = \sqrt{F_x + F_y} \quad (5)$$

A displacement amplitude $|G(i\omega)|$ (Appendix A) is plotted in Figure 4 over the frequency ratio ω/ω_n for different values of damping ratio. For very low frequencies, the amplitude ratio is nearly zero since the unbalance forces are small. As the shaft speed increases, the amplitude shows a large peak near $\omega/\omega_n = 1$, when ω is near the resonance frequency of the system. As discussed above, there is a direct relationship between bearing loads and rotor disk displacements; therefore, the load amplitude F_{OS} over the frequency behaves similarly to the amplitude displacement $|G(i\omega)|$.

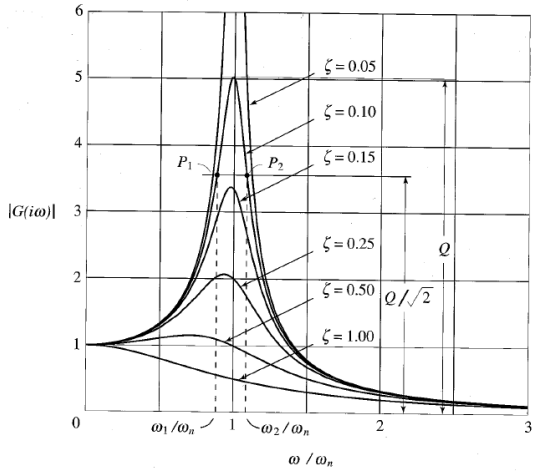

Figure 4. Amplitude response over frequency. (Meirovitch, 2001).

Under the assumption that the rotor disk does not affect the stiffness of the massless shaft, the lateral bending stiffness at the axial center of a simply supported uniform beam is given by:

$$k_s = \frac{48EI}{L^3} \quad (6)$$

where E is the elastic modulus of the shaft, L is the length between the bearings, and I is the shaft area moment of inertia, which can be expressed as follows:

$$I = \frac{\pi D^4}{64} \quad (7)$$

where D is the shaft diameter.

parameter	value	description
$M\ [kg]$	25	rotor disk mass
$D\ [mm]$	20	shaft diameter
$L\ [mm]$	470	shaft length
$E\ [Mpa]$	245000	elasticity modulus
$e\ [mm]$	10	eccentricity
ζ	0.15	damping ratio

Table 1. Dimensions and mechanical data parameters of the experimental test facility

The mentioned model is adapted to the experimental test facility in the lab, which was built especially for this study. Therefore, geometric dimensions and other mechanical data (shown in Table 1) were inserted as inputs to the model. By integrating these parameters to the expressions mentioned above, the lateral bending stiffness was found to be $k_s \cong 9 \cdot$

10^5 $[N/m]$, and the natural frequency of the critical machine is $\omega_n \cong 30$ $[Hz]$.

2.2. A modified L10 bearing life model with ISO factor for variable operating conditions

In this section, a modified L_{10} life statistical model with a_{ISO} factor, which appears as the "life model select" block in Figure 2, is described and developed. An expression for the bearing life is presented (ISO 281, 2007; Harris & Kotzalas, 2006):

$$L_{ISO} = A_1 A_{ISO} \left(\frac{C}{F_e}\right)^p \tag{8}$$

where L_{ISO} is the bearing life in millions of inner ring revolutions, C is the dynamic load capacity, F_e is the external equivalent load (combination of axial and radial load), p is the constant exponent ($p = 3$ for ball bearings and $p = 10/3$ for cylindrical bearings), A_1 is the reliability factor and A_{ISO} is the life ISO factor. If the speed of the inner ring (ω) is known, the L_{ISO} can be expressed in hours:

$$L_{ISO} = A_1 A_{ISO} \frac{10^6}{60\omega} \left(\frac{C}{F_e}\right)^p \tag{9}$$

The ISO 281 standard (2007) determined that A_1 factor can be calculated according to:

$$A_1 = 0.95 \left(\frac{\ln\left(\frac{100}{s}\right)}{\ln\left(\frac{100}{90}\right)}\right) \tag{10}$$

where s is the reliability. In most cases, the accepted reliability is $s = 0.9$ (90% reliability), where in that case $A_1 = 1$. The expression for the modified ISO factor A_{ISO} is:

$$A_{ISO} = 0.1 \left[1 - \left(x_1 - \frac{x_2}{k^{e1}}\right)^{e2} \left(\frac{C_L F_{lim}}{F_e}\right)^{e3}\right]^{e4} \tag{11}$$

where $x_1, x_2, e_1, e_2, e_3, e_4$ are constants that can be found in Harris and Kotzalas (2006), k is the viscosity ratio factor, C_L is the contamination factor and F_{lim} is the load limit that can be found in bearing catalogues (expressions for k, C_L are presented in Appendix B).

In the case that the load and speed profiles are not constant during the bearing operation, the life calculation with Equation 8 or Equation 9 is no longer valid, since it calculates bearing life only with fixed-in-time parameters. However, with the Miner method (1945), an equivalent life-time with variable operating conditions can be calculated. The Miner rule states that where there are k different load magnitudes in a spectrum, each contributing n_i cycles, then if L_i is the number of revolutions to failure of the i^{th} constant load, a failure will occur when:

$$\sum_{i=1}^{k} \frac{n_i}{L_i} = 1 \tag{12}$$

In other words, when the damage accumulation reaches 1, there is a fault in the bearing. In the case that load and speed of bearing are periodic in time, a 'Duty Cycle' can be defined as load or speed profiles in one cycle with length T (in time) or length N_{DC} (in revolutions). An expression for equivalent life can be written (Budynas & Nisbet, 2008):

$$L_{eq} = \frac{1}{\frac{U_1}{L_1} + \frac{U_2}{L_2} + \cdots + \frac{U_i}{L_i}} \tag{13}$$

The methodology assumes the loading history to be composed of thin slices of loading condition, and within each loading slice the rotation speed may be different from others. The ratio between the number of revolutions required for the i^{th} load (F_i) and the number of revolutions in one complete Duty Cycle is defined as a non-dimensional life fraction, which is calculated as follows:

$$U_i = \frac{n_i}{N_{DC}} = \frac{\omega_i \cdot \Delta t_i}{\sum_{i=1}^{k} (\omega_i \cdot \Delta t_i)} \tag{14}$$

2.3. Life model by Tallian

A rolling bearing spalling fatigue life model (Tallian, 1999), which appears as the "life model" block in Figure 2, is described and developed in this section. This model covers rolling contacts under operating conditions varying along the rolling track and time-variable conditions.

The model recognizes three families of defects in the stressed volume: (a) subsurface defects, (b) local surface defects and (c) the "surface distress" micro-spalls. Each defect population is incorporated into a hazard factor describing that population. Hazard factors designated Φ_{2i} measure the severity of these defect families. The overall stress level under which the contact operates is measured by hazard factor Φ_4. The specific characteristics of the stress field are characterized by hazard factors designated Φ_{3i}. Factors Φ_{1i} are model constants. The model-predicted 10% life quantile is:

$$N_{10} = 12AM^{-\frac{1}{\beta}} \left[N_{LP}^{-\frac{1}{\zeta}} \tilde{\Psi}^{\frac{1}{\beta\zeta}} - \tau_0 \Phi_{0LP}^{\frac{1}{\beta\zeta}}\right]^{-\zeta} \tag{15}$$

Where M is the matrix susceptibility factor of material, A is the scaling multiplier, Φ_{0LP} is the baseline matrix susceptibility factor, τ_0 is a fatigue limit stress and the exponents ζ and β are constants. N_{LP} is the Lundberg-Palmgren rating life, which can be obtained by any of the classical methods applicable to space- and time-variable operating conditions, as described, for example, in Harris and Kotzalas (2007). The equivalent hazard factor ratio, $\tilde{\Psi}$, calculated over one Duty Cycle, $\tilde{N}$, is defined as:

$$\tilde{\Psi} = \frac{\tilde{\Phi}_T}{\tilde{\Phi}_{TLP}} \tag{16}$$

With the equivalent hazard factor product $\tilde{\Phi}_T$:

$$\tilde{\Phi}_{\mathrm{T}} = \beta \tilde{N}^{-\beta}$$
$$\sum_{j=1}^{q}\left\{\sum_{k=1}^{m}\left[\Phi_{4,k,j}\sum_{i=a,b,f}(\Phi_{1\mathrm{i}}\Phi_{2\mathrm{i}}\Phi_{3\mathrm{i}})\right]\Delta l N_j^{\beta-1}\right\}\Delta N \tag{17}$$

and the Lundberg-Palmgren hazard factor $\tilde{\Phi}_{TLP}$:

$$\tilde{\Phi}_{TLP} = \beta \tilde{N}^{-\beta}\Phi_{2bLP}\Phi_{3bLP}$$
$$\sum_{j=1}^{q}\left\{\sum_{k=1}^{m}(\Phi_{4LP,k,j})\Delta l N_j^{\beta-1}\right\}\Delta N \tag{18}$$

where q is the number of increments ΔN in the duty cycle ($\tilde{N}$), m is the number of intervals Δl along the rolling track (l), N is the revolution count, Φ_0 is the matrix susceptibility factor, Φ_{2bLP} is the baseline inclusion defect factor and Φ_{3bLP} is the baseline subsurface stress field factor.

As shown above, the model covers life prediction for conditions in which operating parameters may vary along the rolling tracks as well as in time, with the limitation that the time variability can be arbitrary within a relatively short duty cycle but repeats periodically from one duty cycle to the next. Under the variable operating conditions, hazard factors are calculated for short finite intervals along the rolling tracks and for increments of time over which conditions are considered constant. These factors are combined at each interval and then summed over the duty cycle to produce equivalent values $\tilde{\Phi}_{\mathrm{T}}$.

All parameter calculations, constants and default values that are mentioned above can be found in Tallian (1999).

2.4. Transfer functions selection for analysis

In this section, different transfer functions (the "Transfer Function" block in Figure 2) are proposed and discussed. The role of the transfer function is to translate the parameters of attack acting on the critical system (for example, loads, speeds or torque parameters) to an effective function of external load acting on the fuse bearing.

An effective transfer function is defined as a function which increase significantly the life degradation rate of the fuse bearing in case of harmful operating conditions in the critical system relative to normal operation. The bearing type and the transfer function of the fuse system, are examined. The fuse bearing acts as a weak mechanism in the critical system, and hence need to be a small bearing relative to the critical bearings, that fails within a relatively reasonable time. The bearing chosen to be used as the fuse is an SKF 61906 ball bearing, while the bearings of the 'critical' system are SKF 6208 (Appendix B).

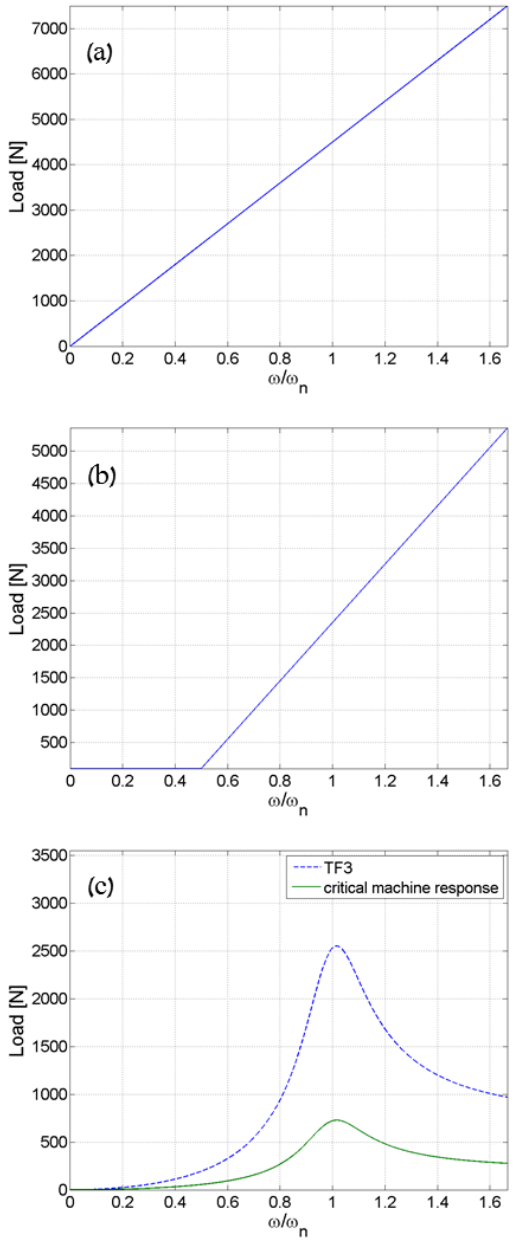

Figure 5. Transfer functions as a function of $\omega/\omega_{\mathrm{n}}$ (a) TF1-linear from the origin, (b) TF2-linear, (c) TF3-proportional to critical machine load.

Three transfer functions are examined and shown in Figure 5. At the current analysis, only the rotating speed profile was chosen to be considered as parameter of the transfer function. The transfer functions get the speed as an input, and translate it to an external load that is applied on the fuse bearing. The first transfer function (a) is a linear function starting from the origin, with a slope of $m = 2.5$. The second transfer function (b) is also linear with the same slope, but not starting from the origin, and the third transfer function tested (c) is similar

to the behavior of the load of the critical machine, multiplied by a factor ($A = 3.5$).

The load is expressed as a function of the frequency ratio ω/ω_n in all transfer functions, but only TF3 function is sensitive to the natural frequency, ω_n, of the critical machine.

3. SIMULATION RESULTS AND DISCUSSION

This chapter presents the results for a number of examples of attack simulations on a critical machine together with the fuse system. An analysis of the results is then performed in order to decide which of the transfer functions provides the best "defense".

3.1. Attack profiles assumptions

To define the nature and form of the profiles of the attack scenarios, some assumptions are made:

1. The attack is defined as an arbitrary speed profile $\omega(t)$ and acts on the critical system and on the fuse system simultaneously.
2. The speed profile, presented as the "profile of attack", repeats periodically from one duty cycle to the next.
3. Proper system operating is defined as an operation speed that is low enough compared to the natural frequency of the 'critical system' ($\omega_n \cong 30\ [Hz]$). For convenience, in a regular operation situation, the speed of the system was selected to be $\omega_0 = 1100\ [rpm] = 18.3\ [Hz]$.
4. The loads acting on critical system bearings are applied only as a result of dynamic responses of the rotating system (section 2.1).
5. The load acting on the fuse bearing is applied as a result of the external load that is created by the applied (selected) transfer function (section 2.4).
6. It is true that cyber-attacks can damage many mechanical parts, but the assumption is that bearings are the weakest part in most of mechanical rotating machines, and as a result, this analysis focuses on bearing failures.

3.2. Defining characteristics of the attack profile

The attack can appear as short and high rotation speed peaks. Each peak form is periodic in time (Figure 6.a), therefore by looking at the profile of one peak cycle (Figure 6.b), three characteristics of the peak profile can be defined. The first characteristic of the peak profile is its amplitude, the second is the width of the peak and the last is the cycle length of one peak.

The analysis carried out allows us to examine how these charasteristics of the attack profile and their forms affect the bearing life of a critical system. In addition, it allows us to examine how each transfer function (Figure 5) reacts to each attack scenario and, as a result, on the fuse bearing life.

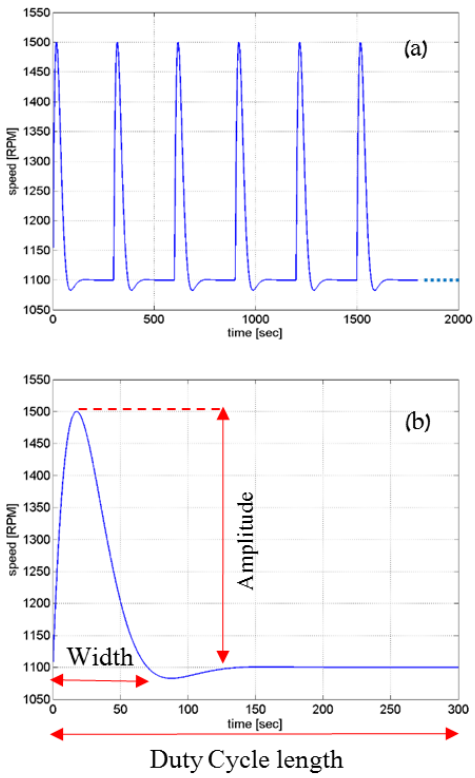

Figure 6. (a) Profile of attack. (b) One cycle of the profile of attack.

3.3. The effect of peak amplitude

The first characteristic of attack profile is analyzed with a set of different sized peak amplitudes (Figure 7). All peaks in the set are with the same size of peak width and same length of duty cycle (Table 2).

Peak amplitude set [rpm]	Peak width [sec]	Duty cycle length [sec]
0-1500	20	300

Table 2. Parameters of peak profile.

It should be noted that the peak amplitude values are defined as the difference between the maximum peak value and the constant rotating speed ω_0. Each peak profile in the set is used as input to the model described in Figure 2, which calculates the life time of the bearings according to two life models (modified L10 model and the Tallian life model).

Figure 8.a and Figure 8.b represent the bearing life results obtained using a modified L10 life model (section 2.2), and the results obtained using the Tallian's life model (section 2.3) respectively. Each bearing life result is normalized by the bearing life at "regular operation" ($\frac{N^i}{N^{reg}}$) and represented as a function of speed profiles with different peak amplitudes. The results show, in both graphs, that the

normalized bearing life curves of the critical machine (full line) decreases with an increase in peak amplitude; but, after a certain point of peak amplitude, the normalized bearing life curve increases moderately. The minimum point of the curve indicates the critical situation in which the system worked under a state of resonance. The logical explanation for the increase after the minimum point is due to the fact that the peak amplitude is moving away from the system's natural frequency, resulting in lower load amplitudes.

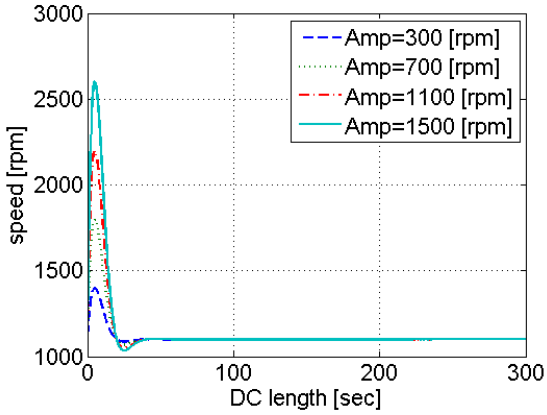

Figure 7. One duty cycle of the profiles of attack used for analysis of peak amplitude effect.

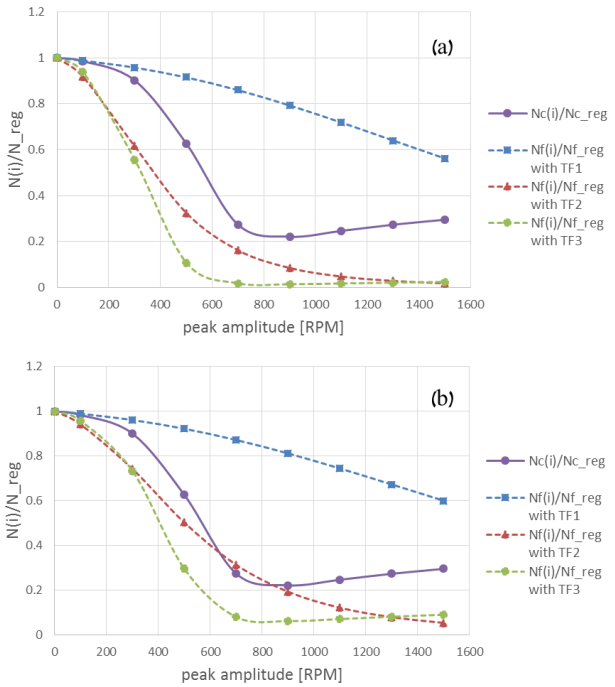

Figure 8. Simulation results under set of profiles with different peak amplitudes (a) using the L10 life model, (b) using the Tallian life model.

Three additional curves (dotted lines) are presented. Each curve belongs to another transfer function mentioned in section 2.4. As with the results of the normalized critical bearing life, these curves describe the normalized bearing life of the fuse bearing. The simulation results show that in most cases, the normalized fuse bearing life decreases with an increase in peak amplitude, for all transfer functions tested. Also noticed was that the biggest degradation occurs with TF3.

3.4. The effect of peak width

The second characteristic of attack profile is analyzed with a set of different sized peak widths (Figure 9). All peaks in the set have the same peak amplitude and same length of duty cycle (Table 3).

Peak amplitude [rpm]	Peak width set [sec]	Duty cycle length [sec]
500	0-60	300

Table 3. Parameters of peak profile.

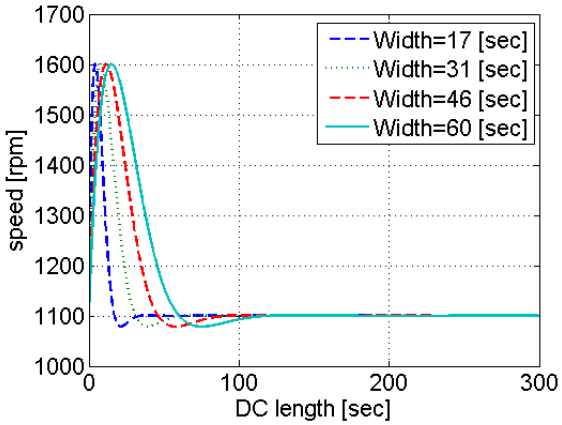

Figure 9. One duty cycle of the profiles of attack used for analysis of peak width effect.

Figure 10.a and Figure 10.b represent the results, using a modified L10 life model, and the Tallian's model for a simulated set of peak widths at the speed profile, respectively. As with the analysis in section 3.3, each result was normalized by bearing life at regular operation. The results show, in both graphs, that the normalized bearing life of the critical machine curve (full line) decreases with an increase in peak width. Also noticed that with all transfer functions, the normalized life of the fuse bearing (dotted lines) decreases with an increase in peak width.

Compared to the other transfer functions, the third transfer function (TF3) gives the best fuse life degradation response due to the specific attack scenario. The transfer functions TF2 and TF3 have greater life degradation effects relative to the

critical bearing life degradation with an increase in peak width.

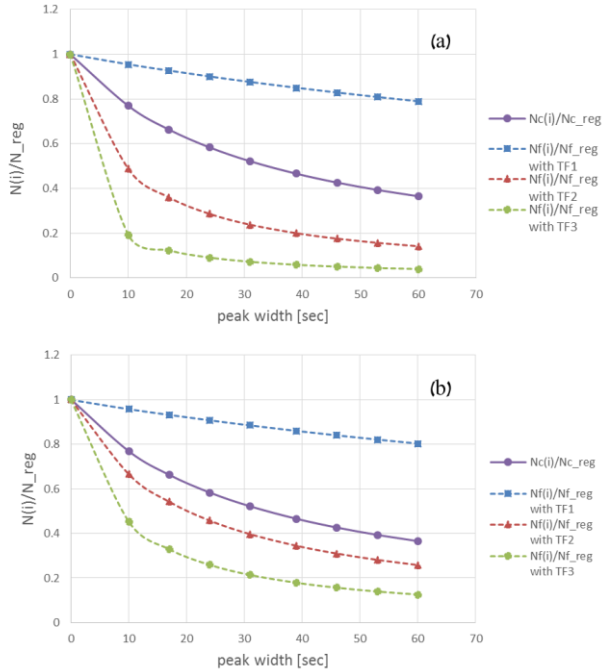

Figure 10. Simulation results under set of profiles with different peak widths (a) using the L10 life model, (b) using the Tallian life model.

3.5. The effect of peak duty cycle length

The third characteristic of attack profile is analyzed with a set of different duty cycle lengths. All peaks in the set have the same size of peak amplitude and same size of peak length (Table 4).

Peak amplitude [rpm]	Peak width [sec]	Duty cycle length set [sec]
500	20	100-10000

Table 4. Parameters of peak profile.

Figure 11.a and Figure 11.b represent the normalized bearings life results ($\frac{N^i}{N^{reg}}$) as a function of speed profile with different duty cycle lengths, for both life models (modified L10 and the Tallian, respectively). It should be noted that the shorter duty cycle length means that the peaks occur more frequently. The results show, in both graphs, that the normalized bearing life of a critical machine curve (full line) decreases with a shorter duty cycle length. Also noted is that with all transfer functions, the normalized life of the fuse bearing (dotted lines) decreases with the shorter duty cycle length. The simulation results are presented in a different form than the other analysis results, since the x-axis in the plots of the normalized degradation trends is in opposite direction. The figures below show a zoom into the interesting part of the curves. Far beyond these scales, all the curves coincide. Compared to the other transfer functions, the third transfer function (TF3) gives the best fuse life degradation response. In this profile character analysis, the transfer functions TF2 and TF3 have greater life degradation effects relative to the critical bearing life degradation.

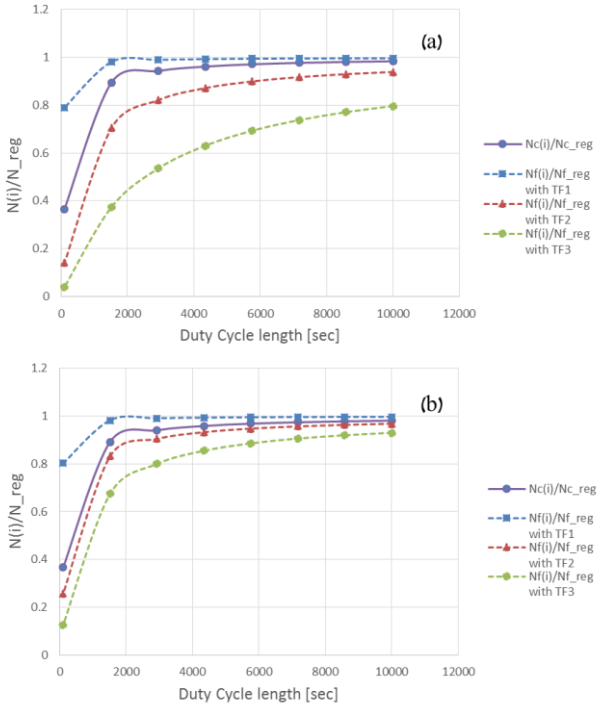

Figure 11. Simulation results under set of profiles with different duty cycle lengths (a) using the L10 life model, (b) using the Tallian life model.

3.6. Optimal Transfer Function

All simulation results show that the fuse bearing life degradation is, to some extent, accelerated with all transfer functions that were considered. In all cases, the third transfer function (TF3) is the most effective when the peak of speed or any speed profile is close to the first natural frequency zone of the critical system. If it is assumed that the most dangerous situation is when the system works near the natural frequency, TF3 is the best solution. In all simulations, TF2 and TF3 have a greater effect on fuse bearing life degradation relative to the critical bearings degradation, which is important for early attack detection, before serious damage is caused to the critical machine bearings. Many mechanical rotating machines also work with standard speeds that are far beyond the natural frequency (areas that do not place the machine in danger), where the vibrations are much lower than in a resonance situation. In that case, using TF3 results in much lower loads on the fuse bearing prevents its early

failure and false alarms. No analysis was done for cases in which the system works at extreme speeds.

4. EXPERIMENTS

An experimental test facility was designed and built especially for this research (Figure 12), including a bearing kit directly connected to an electric motor, simulating the 'critical system'. Another kit representing the 'fuse bearing' kit is located in parallel to the first kit. A fuse bearing is located in the center of the shaft, while the external radial load is applied by a pneumatic piston.

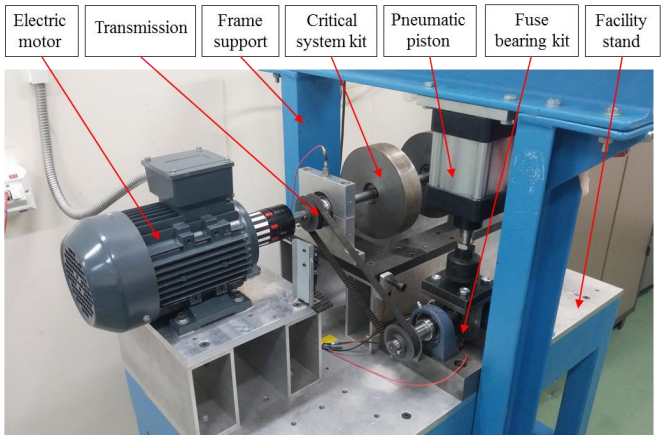

Figure 12. Experimental test facility.

The pneumatic piston is connected to an electric pressure regulator that controls the pressure according to the voltage. The first transfer function (TF1), presented in section 2.4, has been implemented in the fuse system unit of the experimental test facility. The implementation of the transfer function is explained in Figure 13. This functionality creates a linear relationship between the external load and the rotational speed. In addition, it operates autonomously, without computer intervention. The other transfer functions have not yet been implemented.

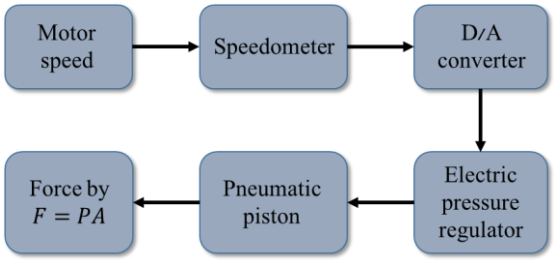

Figure 13. Actual implementation of a linear transfer function in the experimental test facility.

Several fatigue life tests were performed on the fuse bearing with constant rotation speed and external load. These experiments allow the determination of the failure criteria for the fuse bearing selected, which helps to detect early fuse bearing fatigue failures in the future, and also helps to determine the construction of an early faults detection algorithm which will be integrated to the fuse system. The fuse degradation and failure tracking is applied using advanced signal processing and features extraction methodologies. An example of the failure tracking that has been implemented is presented in Figure 14. It shows trend of energy representing the pattern of a damage in the inner race of the fuse bearing as it is manifested in the order spectrum of the vibration envelope. Similar trends are calculated for different patterns representing damages at other locations, i.e. outer race, rotating elements, cage, etc. These trends help to determine the failure criteria of the specific defects. It is noticed that an early inner race defect started to appear after approximately 2300 minutes. A developed inner race defect appeared after 3500 minutes.

In order to demonstrate the model results that have been presented in chapter 3, further experiments should be performed. The experiments will include several attack scenarios, similar to those presented in chapter 3. Speed profile, as a parameter of attack, can be set up through a motor controller or a computer program, to have the desired shape and be periodic in time.

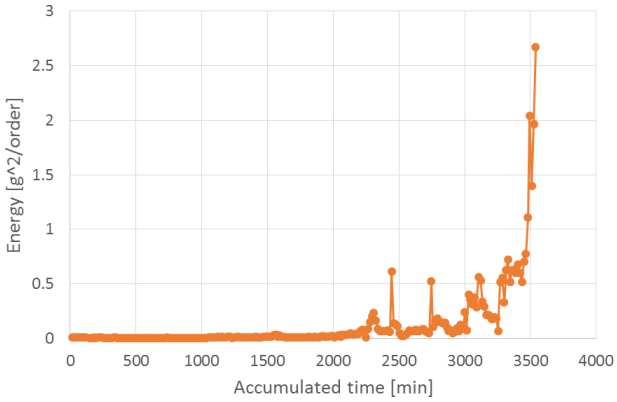

Figure 14. Trend of energy representing a defect on the inner race based on the envelope spectrum.

5. SUMMARY AND CONCLUSIONS

A new concept to cyber protection of critical mechanical rotating machines by a mechanical fuse was presented.

The model objective is to allow the design of the fuse mechanism and to define the requirements for the fuse bearing. The model includes a description of the dynamic behavior of the rotating machine, the transfer function of the loads on the critical component to the fuse bearing, and bearing life estimation models. This model facilitated the analysis of the effect of different transfer functions and attack scenarios.

Three transfer functions were considered, and their capability to accelerate the fuse failure for different attack scenarios was explained. Finally, the simulation results of bearing life-time attacked by several speed attack profiles were presented. The

results show the effects of these profiles on the critical rotating machine and on the fuse system including the transfer function and the fuse bearing. It was concluded that the transfer function that is proportional to the load on the critical system, TF3, was the most sensitive to the set of attacks simulated and, as a result, is the optimal transfer function. It was also shown that both life models have similar behavior under the simulated attack scenarios.

The experimental test facility design, the experiment results and the actual implementation of the transfer function (TF1) demonstrates the concept. It was also shown that early faults in the fuse bearing are detectable early enough.

In order to consolidate the concept, further research and model extension taking into account other parameters of attack should be explored. More scenarios of attack profiles should be simulated in the model, and endurance experiments with several attack profiles should be performed.

ACKNOWLEDGEMENTS

We would like to thank Perlston Foundation for the support of the research.

REFERENCES

L. Meirovitch, Fundamentals of Vibrations, McGraw-Hill Book Company, New York, (Second Printing, 2003), International Edition, McGraw-Hill International Editions, Singapore, 806 pgs. 2001.

International Organization for Standards, International Standard ISO 281, Rolling bearings- dynamic load ratings and rating life, 2007.

Harris, Tedric A., and Michael N. Kotzalas. Advanced concepts of bearing technology: rolling bearing analysis. CRC Press, 2006.

M. A. Miner, Cumulative damage in fatigue. J. appt. Mech. 12, Al.59Al64 (1945).

Richard G. Budynas - J. Keith. Nisbett - Shigley's Mechanical Engineering Design - Boston - McGraw-Hill - 2008 - 8th Ed.

T.E. Tallian, Data fitted bearing life prediction model for variable operating conditions, Tribology Transactions 42(1999) 241.

BIOGRAPHIES

Evyatar Cohen was born in 1986 and currently lives in Beer Sheva city, Israel. He has obtained his first degree in Mechanical Engineering (2013) at the Ben Gurion University of the Negev, where he is currently doing his Master degree. The focus of his research is on promotion of the new concept of cyber defense that is the subject of the current paper, and also on characterizing of bearings life degradation through vibration analysis.

Prof. Jacob Bortman joined the academic faculty of BGU in September 2010 as a full Professor. He spent thirty years in the Israel Air Force (IAF), retiring with rank of Brigadier General. In the IAF he held the following positions: Head of the Fatigue and Damage Tolerance Lab; Head of the UAV (unmanned aerial vehicle) and Space Department; Head of the the IAF's Engineering Laboratories; Head of the Aircraft Department, and finally Head of the Material Directorate, a senior position which reports directly to the chief commander of the IAF. He received all three of his academic degrees in Mechanical Engineering. He received his D.Sc. degree from Washington University in 1991. His areas of research in the Dept. of Mechanical Engineering include: Health usage monitoring systems (HUMS), Conditioned based maintenance (CBM); Usage and fatigue damage survey; Finite Element Method; and Composite materials.

Renata Klein received her B.Sc. in Physics and Ph.D. in the field of Signal Processing from the Technion, Israel Institute of Technology. In the first 17 years of her professional career, she worked in ADA-Rafael, the Israeli Armament Development Authority, where she managed the Vibration Analysis department. In the next 14 years, she focused on development of automatic health management systems for machinery. She invented and managed the development of vibration based diagnostics and prognostics systems that are used successfully by the Israeli Air Force in its combat helicopters and UAV fleets, and by leading jet engine manufacturers. Renata is a lecturer at the faculty of Mechanical Engineering in Ben Gurion University of the Negev, where she supervises research in the area of vibration based Diagnostics and Prognostics. In the recent years, Renata is the CEO and owner of "R.K. Diagnostics", providing R&D services and algorithms to companies who wish to integrate machinery health management and prognostics capabilities in their products.

APPENDIX A

The sizes $|X(\omega)| = |Y(\omega)|$ so

$$|X(\omega)| = e\left(\frac{\omega}{\omega_n}\right)^2 |G(i\omega)| \tag{A1}$$

While $|G(i\omega)|$ is

$$|G(i\omega)| = \frac{1}{\left\{\left[1-\left(\frac{\omega}{\omega_n}\right)^2\right]^2 + \left(\frac{2\zeta\omega}{\omega_n}\right)^2\right\}^{0.5}} \tag{A2}$$

And the phase ϕ

$$\phi = \tan^{-1}\frac{2\zeta\omega/\omega_n}{1-\left(\frac{\omega}{\omega_n}\right)^2} \tag{A3}$$

APPENDIX B

The k viscosity factor ratio is calculated by:

$$k = \frac{v}{v_1} \tag{B1}$$

While v is the actual viscosity factor that depends on grease temperature and v_1 is the viscosity factor desired for proper separation between contacts, which is calculated by:

$$v_1 = \begin{cases} 45000 \cdot n^{-0.83} d_m^{-0.5} & for\ n < 1000\ [rpm] \\ 4500 \cdot n^{-0.5} d_m^{-0.5} & for\ n \geq 1000\ [rpm] \end{cases} \tag{B2}$$

The contamination factor C_L is expressed by:

$$C_L = min(C_{L1} \cdot k^{0.68} \cdot d_m^{0.55}, 1) \cdot \left(1 - \frac{C_{L2}}{\sqrt[3]{d_m}}\right) \tag{B3}$$

While d_m is the mean diameter of the bearing. $C_{L1}\ and\ C_{L2}$ are contamination constants that can be found in Harris's book.

The properties of the bearings selected are listed below:

Bearing	C $[kN]$	Inner diameter d $[mm]$	Outer diameter D $[mm]$	Width B $[mm]$	F_{lim} $[kN]$
SKF 6208 'critical'	32.5	40	80	18	0.8
SKF 61906 'fuse'	7.28	30	47	9	0.212

Table 5. Model bearing properties.